Achievement of low temperature superplasticity in a commercial aluminum alloy processed by equal-channel angular extrusion

F. Musin[1], R. Kaibyshev[1], Y. Motohashi[2], G Itoh[2]

[1]Institute for Metals Superplasticity Problems, Ufa, Russia, fanil@anrb.ru
[2]Ibaraki University, Hitachi, Ibaraki, Japan, motohasi@mech.ibaraki.ac.jp

Keywords: aluminium alloys, low temperature superplastic deformation, microstructure, intense plastic straining, ultra-fine grain size

Abstract. A commercial Al-4.1%Mg-2.0%Li-0.16%Sc-0.07%Zr alloy was used as a starting material. The submicrocrystalline structure with an average grain size of about 0.8 μm was developed by equal-channel angular extrusion. Superplastic behavior of this alloy was examined in the temperature range 150-250°C at strain rates ranging from $1.4\text{x}10^{-5}$ to $5.6\text{x}10^{-2}$ s^{-1}. A maximum elongation-to-failure of 440% was recorded at 175°C ($0.5T_m$, where T_m is the melting point) and a strain rate of $2.8\text{x}10^{-5}s^{-1}$. The strain rate sensitivity was measured as ~0.32 at these conditions. This temperature is exceptionally low for superplasticity in Al-based alloys, as it has been reported to date. Features of superplastic deformation at such the low temperature are considered.

Introduction

Superplastic forming is a well-established manufacturing technology for the fabrication of articles with complicated shapes. The high tensile ductilities associated with superplastic flow are generally manifested at temperatures greater than $0.7T_m$, where T_m is the melting point, and at strain rates less than 10^{-3} s^{-1} in aluminum alloys with grain size ranging from 2 to 10 μm [1,2]. These conditions of superplastic forming are the main disadvantages of this technique restricting its commercial applications. The strain rate during superplastic deformation, $\dot{\varepsilon}$, generally obeys the following relationship:

$$\dot{\varepsilon} = A\frac{DGb}{kT}\left(\frac{b}{d}\right)^p\left(\frac{\sigma}{G}\right)^2, \qquad (1)$$

where A is a dimensionless constant, b is the Burgers vector, d is the grain size, σ is the applied stress, G is the shear modulus, k is Boltzmann's constant, D is the grain boundary diffusion coefficient that defines the temperature dependence of the strain rate at constant stress and structure, T is the absolute temperature, and p is the exponent of the inverse grain size that ranges from 2 to 3, if grain boundary sliding dominates the deformation. Since the strain rate in superplasticity is inversely proportional to the square or cube of the grain size, a decrease in the grain size leads to a shift of the superplasticity interval to higher strain rates or lower temperatures. Both of these trends would be beneficial for industrial forming processes because they provide a potential to produce complex parts more rapidly and at a lower forming temperature, where the tool costs are reduced. In addition, the lower forming temperatures can also be utilized for reducing the surface oxidation and preventing the depletion of alloying elements. The latter is particularly important for aluminium alloys containing lithium that exhibits a high rate of vaporization from the surface layer at elevated temperatures [3,4].

Recently it has been shown that the grain size in aluminum alloys may be significantly reduced by imposing an intense plastic strain through the process of equal-channel angular extrusion (ECAE), which is the most popular laboratory procedure [5-9]. Aluminum alloys having such a fine microstructure are capable of exhibiting superplastic ductilities at higher strain rates or lower temperatures. It has been recently reported that the Al-Li-Mg-Sc-Zr alloy designated in the Former Soviet Union as the 1421 aluminium alloy, subjected to ECAE resulting in an average grain size of

~1 μm exhibits the highest elongation (>1850%) at a temperature of 400°C and a strain rate of $1.4x10^{-2}$ s^{-1} [10].

The present work is a continuation of studies on the 1421 aluminum alloy with intent to evaluate its potential for superplasticity at low temperatures. The main attention is focused on an evaluation of the lower temperature limit for the manifestation of superplasticity in this material. The second objective of the paper is to provide a direct comparison of the superplastic behaviors of the 1421 alloy at high and low temperatures.

Material and Experimental Procedure

The alloy used in the present study was the commercial grade 1421 aluminum alloy, denoted as 1421 Al herein, with a chemical composition Al-4.1%Mg-2.0%Li-0.16%Sc-0.07%Zr (in weight %). Details of solution treatment as well as ECAE processing of the alloy have been described earlier [10].

Tensile specimens were cut parallel to the longitudinal axis of the pressed rods with a gauge length of 6 mm and cross-section of 1.5x3 mm^2. These samples were pulled in tension to failure in air using a Shimadzu universal testing machine (Model AG-G-20kN) operating at a constant cross-head speed. Tension tests were carried out in the temperature interval 150-250°C at strain rates ranging from $1.4x10^{-5}$ to $5.6x10^{-2}$ s^{-1}. Temperature accuracy was within ±2°C. The values of the strain rate sensitivity were determined by strain-rate-jump tests [1,2]. The magnitudes of the elongation to failure were measured by using two scratches within a gauge section of samples.

All structural studies were carried out on the longitudinal (tension) and long transverse sections of the specimens. The microstructures were examined using Neofot-32 optical microscope and JEOL JSM-840A scanning microscope equipped with an electron backscattered diffraction (EBSD) hard- and software provided by Oxford Instruments, Ltd. Cavitation was evaluated by the standard point-count technique.

Results

Figure 1a shows a typical EBSD map of the starting 1421 Al after ECAE pressing. It is evident that equiaxed grains with an average size of ~0.8 μm are outlined by high angle boundaries, and the fraction of high-angle boundaries (θ≥15 deg.) was found to be about 80% (Fig.1b). A careful examination of many areas showed that the microstructure of the ECAE processed 1421 Al is reasonably homogeneous on a macroscopic level, although stringers of secondary phase, mainly of S-phase, can be found [10]. Grain boundaries exhibit well-defined extinction contrast indicating on their equilibrium state (Fig.1c); grain boundary and lattice dislocations were rarely observed.

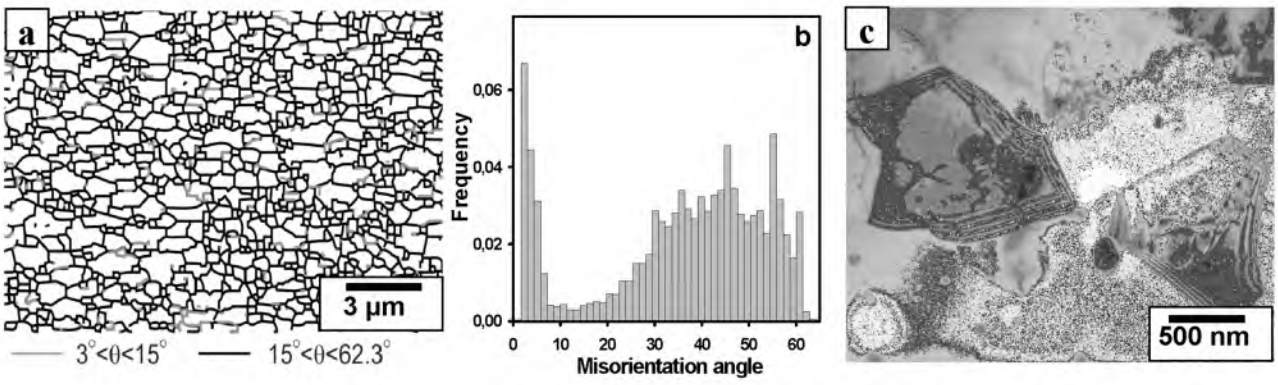

Fig.1. Microstructure of the 1421 subjected to ECAE at 325°C to a total strain of 16. (a) EBSD map, (b) misorientation distribution and (c) TEM micrograph.

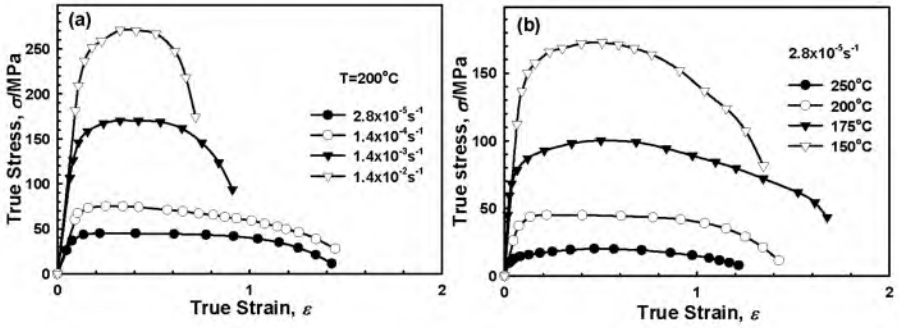

Fig. 2. True stress vs true strain for the samples tested (a) at 200°C and different initial strain rates; (b) at $\dot{\varepsilon}$ =2.8x10^{-4}s^{-1} and different temperatures.

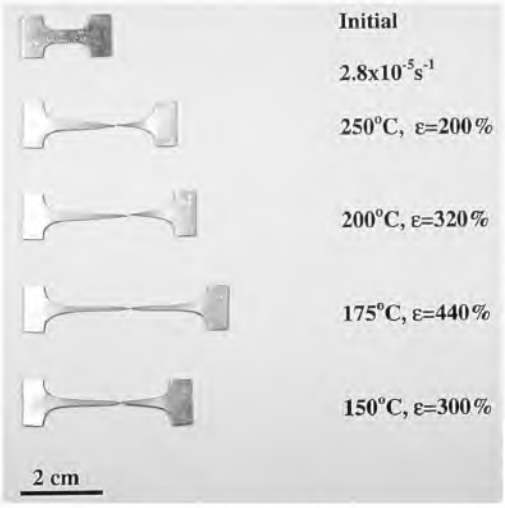

Fig. 3. Samples of the 1421Al after ECAE and pulling to failure at different temperatures and 1.4x10^{-2}s^{-1}.

Mechanical properties. Typical true stress – true strain curves for the ECAE processed 1421 Al at a fixed temperature of 200°C and strain rates ranging from 2.8x10^{-5} to 1.4x10^{-2}s^{-1} and at an initial strain rate of 2.8x10^{-5} s^{-1} and temperatures ranging from 150°C to 250°C are shown in Fig.2a and b, respectively. It is seen that significant strain hardening takes place initially followed by steady-state flow after which the flow stress continuously decreases until fracture. The steady-state tends to shorten with increasing strain rate or decreasing temperature. Concurrently, increasing temperature or decreasing strain rate leads to a reduction in the initial work hardening. The specimens before and after testing at a strain rate of 2.8x10^{-5}s^{-1} and various temperatures are shown in Fig.3. In all examined conditions, fracture occurs by a well-defined unstable plastic flow [2]. However, at T≤200°C, plastic deformation within the gauge section is reasonable uniform.

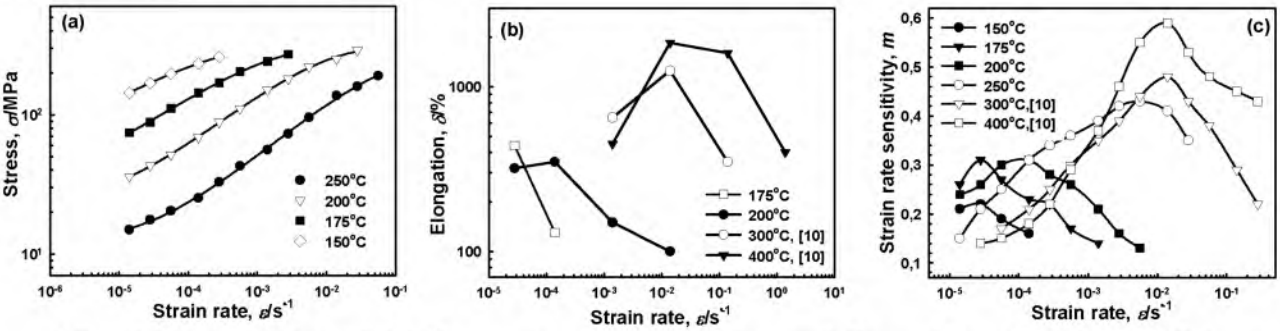

Fig. 4 The variation of (a) flow stress, (b) elongation-to-failure, δ, and (c) the coefficient of strain rate sensitivity, m, with strain rate. Datum points for temperatures of 300 and 400°C [10] are also included in Fig.4b and c.

The flow stress taken at a true strain of ~0.4 is plotted in Fig.4a as a function of strain rate. Apparently, at T≥175°C, the 1421 Al exhibits a sigmoidal relationship between the flow stress and strain rate and the three well-known regions of superplastic deformation [1,2] can be identified. At T=150°C, the stress-strain rate curve does not exhibit a sigmoidal shape. Elongation-to-failure, δ, and the strain rate sensitivity coefficient, m, are plotted in Fig.4b&c as a function of strain rate. The highest values of the strain rate sensitivity coefficient and elongation-to-failure appear in the Region 2 (Figs. 4b&c). At 175°C, the maximum value of elongation to failure (~440%) appears at the slowest strain rate, where the strain rate sensitivity coefficient is equal to 0.32. An increase in temperature leads to a shift of the optimal strain rate for superplasticity, $\dot{\varepsilon}_{opt}$,

at which the highest values of strain rate sensitivity and ductility are reached , to higher magnitudes; the optimal strain rate region for superplasticity (i.e. Region 2) expands. At temperatures greater than 250°C, the highest *m* value (m~0.5) occurs at a strain rate of $1.4x10^{-2}s^{-1}$, at which the elongation to failure exceeds 1000% in a wide temperature range [10].

Microstructural evolution. Superplastic deformation does not lead to remarkable grain growth and cavitation at optimal condition for superplasticity at low temperature (Fig 5a). An average grain size slightly increases from ~0.8 μm to ~1.1 μm. An elongation of the grains in the tension direction with an aspect ratio of ~1.3 was found. The AR value is typical for conventional superplastic alloys, where a high contribution of grain boundary sliding to the total elongation takes place [1,2].

Examination of the unetched surface of the specimen pulled to failure at 175°C showed that the cavities are located along the coarse S-phase inclusions [10] forming stringers along the tension direction (Fig.5b). It is known [2] that such cavities nucleate at the hard particle/metal interfaces. This can be attributed to the limited ability of the Al_2FeSi-phase to contribute to the accommodation of grain boundary sliding (GBS). The volume fraction of cavities was 1.5%.

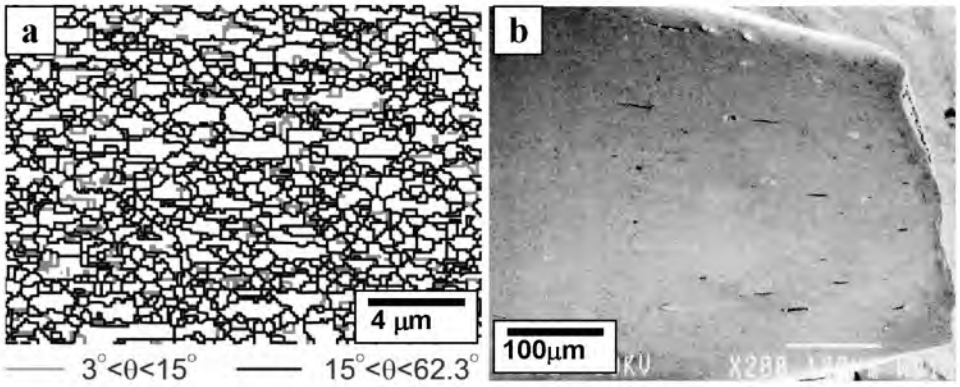

Fig. 5. Microstructure of the 1421Al after tension test at the temperature of 175°C and the strain rate of $2.8x10^{-5}s^{-1}$. (a) EBSD map, (b) SEM. Only limited cavitation is observed in (b).

Discussion

Low-temperature superplasticity. A set of experimental data obtained in the present study allows emphasizing features of superplastic behavior of the 1421 Al at low temperatures compared with high-strain-rate superplasticity at T≥250°C [10].

1. A well-defined steady-state flow occurs. At higher temperatures, extensive strain hardening takes place initially. After reaching a maximum stress, the flow stress continuously decreases until fracture. A well-defined peak in flow stress can be observed, and no steady-state flow takes place.
2. Fracture of samples of the 1421 Al occurs by unstable plastic flow at low temperature. At T≥250°C, pseudo-brittle fracture by cavitation took place.
3. The value of coefficient of strain rate sensitivity m~0.33 less than the m value for the majority of superplastic materials (i.e. m≤0.33) [1,2]. At higher temperature, the m value lies in the range from 0.4 to 0.6.

Temperature dependence of the optimum strain rate, $\dot{\varepsilon}_{opt}$, at which the highest value of strain rate sensitivity appears, is presented in Fig. 6. The datum points for 300 and 400°C were taken from Ref. [10]. Evidently, the $\dot{\varepsilon}_{opt}$ value is constant in the low temperature interval of 150-175°C as well as at the high temperature interval of 300-400°C. Decreasing temperature from 300°C to 200°C leads to drop in $\dot{\varepsilon}_{opt}$ of about two orders of magnitude. It is obvious that two distinctly different types of superplastic behavior can be distinguished. Such quite abrupt change in the strain rate, at which the highest m value is observed, can be associated with transition from high temperature superplasticity (HTSP) to low temperature superplasticity (LTSP). At T≥250°C, the 1421 Al exhibits HTSP regime considered in Ref.[10] in detail. The highest values of the strain rate sensitivity coefficient (m~0.5) and elongation-to-failure (δ>1000%) are observed at strain rates greater than 10^{-2} s^{-1}. At T≤200°C, the 1421 Al exhibits LTSP regime; the optimal strain rate for

superplasticity takes place at strain rates lower than 10^{-4} s^{-1}, and the highest m value and the δ value are equal to ~0.3 and ~440%, respectively.

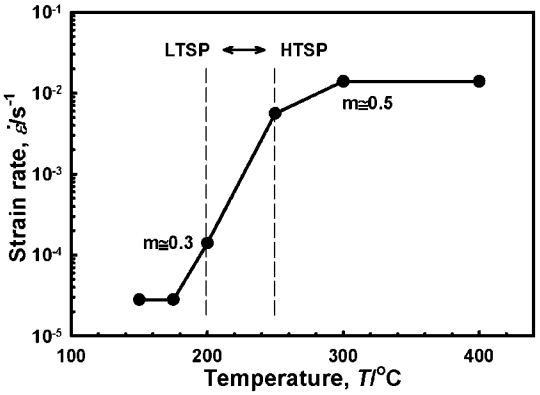

Fig. 6 Temperature dependence of the strain rate, at which the highest value of strain rate sensitivity is observed. Experimental points for 300°C and 400°C were taken from Ref. [10].

It is worth noting that m~0.3 is expected to demonstrate ductilities lower than those observed experimentally in the present study. For instance, an elongation to failure of 440% was recorded at 175°C, while the m value was about 0.3. Since extensive strain hardening takes place at low strain in the low temperature interval 150-200°C and an essentially uniform deformation occurs within the majority of the gauge length (Fig.3), it can be suggested that the visibly stable plastic flow takes place in the region of low strain within the gauge lengths.

Apparently, the strain rate sensitivity coefficient strongly correlates with transition from HTSP to LTSP. It is known that a high strain rate sensitivity confers a high resistance to neck development providing a sharp increase in the flow stress within the necked region, where a high local strain rate takes place [2]. At higher temperatures, the m value is about 0.5 (Fig.5c) and a high tensile ductility associated with the suppression of necking by strain rate hardening is achieved. This m value corresponds to the conventional superplastic region (Region 2) suggesting a high contribution of grain boundary sliding to the total elongation [1,2]. At low temperatures, the strain rate sensitivity coefficient is about 0.3 and the tensile ductility is limited by necking. Thus, superplastic behavior of the 1421 Al is distinctly different at low temperatures compared with its deformation behavior at high temperatures.

It is generally believed that the m=0.3 value corresponds to dominance of dislocation creep over the grain boundary sliding [1,2]. Recently, it was assumed that viscous dislocation glide even could be the dominating deformation mechanism for low temperature superplasticity [11].

Microstructural conditions for manifestation of superplasticity at low temperatures. The results of present study indicate that the 1421 Al exhibits superplastic behavior at very low temperatures, which are used for the second step of aging in the conventional route of heat treatment. In comparison with the other aluminum alloys the 1421 Al demonstrates a high elongation-to-failure of 440% at an exceptionally low temperature of 175°C. In addition, the starting alloy has a relatively coarse grain size of ~0.8 μm compared with aluminum alloys which were found to exhibit superplasticity at T≤250°C.

Thus, it is obvious that equation (1) is valid in a very wide temperature range 175-450°C for the 1421Al, suggesting that GBS is the dominating mechanism for superplastic deformation at low temperature. To support this conclusion the 1421 Al with initial grain size of ~3 μm (which was obtained by ECAE at 400°C) was tested at 175°C and strain rate of $2.8 \times 10^{-5} s^{-1}$. It is seen that the superplastic behavior of the 1421 is strongly dependent on initial grain size. At these conditions, the 1421 Al with a starting grain size of ~3 μm exhibits poor superplastic behavior and elongation-to failure does not exceed 180% with a corresponding m value of 0.23. Decreasing strain rate leads to increasing the m value. It should be noted that the m value in the 1421 Al with grain size of ~3 μm does not achieve a maximum in the investigated strain rate range.

From this point of view, a comparison of present experimental data with those obtained for the 1420 Al [6,7] leads to an ambiguous conclusion. It is obvious that the 1421 Al exhibits larger

elongation-to-failure at lower temperatures than the 1420 Al, despite the significantly larger grain size (~1 μm and ~0.3 μm, respectively). In addition, the flow stress in the 1421Al [10] was essentially the same with that recorded in the 1420 Al at similar conditions of strain rate and temperature. Inspection of structural data reported in Refs. [7] shows that this fact can be attributed to a non-equilibrium state of grain boundaries in the 1420 Al containing a high density of grain boundary defects. It was recently shown that ultrafine grained structures produced by intense plastic straining at low temperatures can exhibit high internal long-range stress fields originated from these defects [12]. Mg alloys in this microstructural condition demonstrate poor superplastic properties [13,14]. However, processing of these Mg alloys at higher temperatures resulting in coarser grain size and highly reduced density of grain boundary defects provides enhanced superplastic properties [13,14]. Therefore, merely achieving a grain size less than 1 μm is not sufficient to guarantee that an aluminum alloy will exhibit low temperature superplasticity, since the grain structure needs to be essentially in an equilibrium state and containing a reasonably low dislocation density [11].

Summary

The present experimental results can be summarized as follows. An ultrafine grain size of ~0.8 μm was obtained in a commercial grade of the Al-Mg-Li-Sc-Zr alloy subjected to ECAE pressing at 325°C to a true strain of 16. Low temperature superplasticity was achieved in the alloy in the temperature interval of 150-200°C. The highest tensile elongation of 440% corresponding with the strain rate sensitivity coefficient m~0.32 was recorded at an initial strain rate of 2.8×10^{-5} s^{-1} and 175°C, which is the lowest temperature for superplasticity in Al-based alloys reported to date.

Acknowledgements

This work was supported in part by the International Science and Technology Center under Project no.2011 and Japan Light Metal Educational Foundation.

References

[1] O.A. Kaibyshev: *Superplasticity of Alloys, Intermetallides, and Ceramics* (SpringerVerlag, Berlin 1992).
[2] J. Pilling, N. Ridley: *Superplasticity in crystalline solids* (The Institute of Metals, London 1989).
[3] J.M. Pafazian, R.L. Schulte and P.N. Adler: Metall. Mater. Trans. Vol. 17A (1986), p. 635.
[4] H.P.Pu, F.C.Liu, J.C.Huang: Metall.Mater.Trans. Vol. 26A (1995), p. 1153.
[5] Z. Horita, M. Furukawa, M. Nemoto, A.J. Barnes and T.G. Langdon: Acta Mater. Vol. 48 (2000), p. 3633.
[6] S. Lee, P.B. Berbon, M. Furukawa, Z. Horita, M. Nemoto, N.K. Tsenev, R.Z. Valiev and T.G. Langdon: Mater.Sci.Eng. Vol. A272 (1999), p. 63.
[7] R.S.Mishra, R.Z.Valiev, S.X.McFadden, R.K.Islamgaliev, A.K.Mukherjee: Phil.Mag.A Vol. 81 (2001), p. 37.
[8] S.Lee, A.Utsunomiya, H.Akamatsu, K.Neishi, M.Furukawa, Z.Horita, T.G.Langdon: Acta Mater. Vol. 50 (2002), p.553.
[9] S.Ota, H.Akamatsu, K.Neishi, M.Furukawa, Z.Horita, T.G.Langdon: Mater.Trans Vol. 43 (2002), p. 2364.
[10] F. Musin, R. Kaibyshev, Y. Motohashi, T. Sakuma and G. Itoh: Mater. Trans. Vol. 43 (2002), p. 2370.
[11] I.C. Hsiao, J.C. Huang and S.W. Su: Metall.Mater.Trans. Vol. 33A (2002), p. 1373.
[12] A. Belyakov, T. Sakai, H. Miura, R. Kaibyshev and K. Tsuzaki: Acta Mater., Vol. 50 (2002), p. 1547.
[13] R.Kaibyshev, A.Galiyev: Suppl. vol. to Superplasticity and Superplastic Forming, TMS, ed. by A.Ghosh, T.Bieler (1998), p. 20.
[14] M. Mabuchi, K. Ameyama, H. Iwasaki and K. Higashi: Acta Mater. Vol. 47 (1999), p. 2047.